Tile: Repetitive Spreading Depolarization induces the activation of cell differentiation, synaptic plasticity and neuroprotective pathways.

Michela Dell'Orco [a], Jordan E. Weisend [a], Nora I. Perrone-Bizzozero [a], Andrew P. Carlson [b], Russell A. Morton [a] , David N Linsenbardt [a] & C. William Shuttleworth [a].

[a] Department of Neurosciences, [b] Department of Neurosurgery; University of New Mexico School of Medicine, Albuquerque, New Mexico, 87131, USA.

Correspondence to:

C. William Shuttleworth, Ph.D.

Department of Neurosciences

1 University of New Mexico, MSC08 4740

Albuquerque, NM 87131

USA

Email:bshuttleworth@salud.unm.edu

Phone: (505) 272 4290

KEYWORDS: spreading depression, preconditioning, gene expression, pathway analysis, brain injury, stroke.

Abstract

Spreading depolarization (SD) is a slowly propagating wave of profound depolarization that sweeps through cortical tissue. While much emphasis has been placed on the damaging consequences of SD, it is possible that SDs also activate compensatory pathways related to cell survival and plasticity. The present study aimed to provide an unbiased assessment of gene expression changes following SD, as well as novel molecular networks associated with these transcriptional alterations. SD clusters were induced with either focal application of KCl or with optogenetic stimulation in healthy mice, and then 2 hours later cortical RNA was extracted and sequenced. SD's significantly increased the expression of 21 genes - no genes were significantly downregulated. Notable top hits included the immediate early genes FOS, ARC, and JUN, the cell proliferation-related gene DUSP6, the plasticity-related gene HOMER1, and inflammation related genes PTGS2, EGR2, and NR4A1. Pathway analysis identified the recruitment of genes associated with axonogenesis, branching, neuritogenesis, and dendritic growth, as well as inhibition of pathways associated with cell death, apoptosis, and neuronal degeneration. These results identify the induction of plasticity and/or circuit modification as an important consequence of SDs in healthy tissue, as well as specific gene targets and pathways amenable to manipulation in follow up studies.

Introduction

Spreading Depolarization (SD) is a slowly propagating wave of extended depolarization that is followed by suppression of neural activity, first described by Leao (Leao 1944). SD is implicated as a mechanism of migraine with aura (Pietrobon and Moskowitz 2014; Charles and Brennan 2009) and otherwise healthy brain is able to fully recover from SD (Nedergaard and Hansen 1988). However, the long duration of depolarization (up to a minute or more) can lead to severe energy depletion (Dreier et al. 2017; Lindquist and Shuttleworth 2014), particularly when coupled with neurovascular disruptions in ischemic brain (Hartings et al. 2017; Ayata and Lauritzen 2015; Dreier 2011). In addition, transient extracellular glutamate surges caused by SD can be sufficient to cause neuronal injury in metabolically compromised brain tissue (Aiba et al. 2012; Hinzman et al. 2015). Recent work has identified SDs as contributors to tissue loss following stroke, trauma, and other acute brain injuries (Dreier et al. 2017; Lauritzen et al. 2011) and initial efforts have begun targeting SD in efforts to improve outcomes in brain injury (Helbok et al. 2020; Carlson et al. 2018).

In contrast to the large body of literature characterizing electrophysiological and vascular responses to SD, only a relatively small number of studies have examined SD-induced gene expression changes and their relationship to outcomes in different experimental and clinical conditions. Initial studies identified increases in brain derived neurotrophic factor (BDNF), c-Fos and heat shock protein 70 (HSP70) (Dietrich et al. 2000; Kokaia et al. 1993; Karikó et al. 1998; Matsushima, Hogan, and Hakim 1996; Rangel et al. 2001). Subsequent studies showed increased expression of pro-inflammatory and apoptotic genes, including tumor necrosis factor (TNF), C-C motif chemokine ligand 2 (CCL2), interleukin-1 (IL-1) and -6, and cyclooxygenase-2 (COX-2), and B-cell lymphoma 2 (BCL-2) (Eising et al. 2017; Jander et al. 2001; Kaido et al. 2012; Takizawa et al. 2020). While most of these studies focused predetermined genes, a relatively recent microarray study has applied gene ontology (GO) and pathway analysis (PA) to the study of SD in rats (Sintas et al. 2017). Pathway analysis allows the identification of altered cellular and molecular

64 pathways from data obtained from high-throughput technologies; leading to the identification of novel sets
65 of related genes that are altered in different conditions (García-Campos, Espinal-Enríquez, and Hernández-
66 Lemus 2015). Sintas and colleagues focused their analysis on SD's influence on pathways linked to
67 oxidative stress and cellular injury, but less is known of other cellular adaptations that may occur. A lack
68 of comprehensive transcriptomic analysis has limited the understanding of potentially beneficial pathways
69 that could be activated following SD.
70
71 In the current study, we provide the first unbiased RNA sequencing (RNAseq) analysis following SD. We
72 applied pathway analysis approaches to uncover candidate networks and novel genes altered by SD. To
73 increase generalizability, we combined data from the two most common methods of SD initiation (focal
74 depolarization with either topical KCl administration or optogenetic stimulation) and generated clusters of
75 SDs that are analogous to patterns of SDs that have been recorded from injured human brain. The results
76 identify the upregulation of multiple molecular pathways that could regulate potentially beneficial effects
77 of SD, such as neuritogenesis and synaptic plasticity.
78
79 **RESULTS**

80 **1) Identification of gene expression induced by repetitive spreading depolarizations**

81 Multiple SDs (4 over a period of 2 hours) were generated to match clusters of SDs in clinical settings (Dreier
82 et al. 2017) and this procedure has previously been shown to induce robust transcriptional changes (Sintas
83 et al. 2017; Urbach, Bruehl, and Witte 2006; Takizawa et al. 2020). Thirty minutes after the last SD or sham
84 stimulus, the neocortex was removed, and RNA extracted from tissue subjected to SD or shams for
85 subsequent RNA sequencing (see Materials and Methods and **Supplementary Figure 1**).

86 As both focal KCl and optogenetic stimulation are routinely used in studies of SD, data from these two SD-
87 stimulation methods were combined for differential expression (DE) analysis here to increase
88 generalizability. For the combined DE analysis, we performed DESeq2 analysis (Ge, Son, and Yao 2018)

89 and identified 26 genes that were also significant after false discovery rate correction (FDR <0.05) when
90 comparing the SD group with the sham tissues (**Figure 1, red, FDR <0.05)**.

91 Consistent with previous studies (Kaido et al. 2012; Rangel et al. 2001; Kokaia et al. 1993; Dietrich et al.
92 2000), we found significant changes intermediate early genes ARC, FOS and JUN proto-oncogenes, and
93 early growth response (EGR) genes. Among other DEGs with significantly increased levels were
94 adrenoceptor beta 1 (ADRB1), dual specificity phosphatase (DUSP) gene family, the nuclear receptor
95 subfamily 4 group A member 1 (NR4A1), and prostaglandin-endoperoxide synthase 2 (PTGS2).

96

97 **2) Molecular networks regulated by repetitive SDs**

98 We next used Ingenuity Pathway Analysis (IPA) to identify molecular networks and biological pathways
99 regulated by DEGs. This information was then used to obtain a prediction of physiological and pathological
100 brain processes altered by SD. **Figure 2A** and **B** show the top two scored networks (score 63 and 36)
101 generated by IPA with the combined DEGs upregulated in the SD group as compared to sham animals. The
102 intensity of the color red for each molecule is proportional to the fold change (FC) of the labeled gene. Full
103 arrows indicate a direct relationship between molecules, while dotted arrows indicate a predicted indirect
104 relationship. Orange arrows indicate the predicted activation of a gene, while yellow indicates predicted
105 inhibition. These networks implicated SD target genes associated with cell proliferation and synaptic
106 activity, including cAMP responsive element binding protein 1 (CREB1), mitogen-activated protein kinase
107 1 and 3 (MAPK1 and MAPK3), and HOMER1 (**Figure 2B**).

108 Predictions of SD-induced changes associated with known disease states and functions are shown in **Figure**
109 **2C** and they include: neurological diseases, psychological disorders, nervous system development and
110 function, tissue morphology, and tissue development. The complete list of diseases and functions and the
111 genes associated with each pathway are reported in **Supplementary Table 2**. **Figure 2C** also shows the
112 number of genes associated with each pathway and associated p value range. They are shown together so

113 that different strengths of the network elements can be compared. A complete list of networks and
114 associated DEGs is reported in **Supplementary Table 3.**

115 **Figure 3** illustrates pathways related to cellular functions induced by repetitive spreading depolarization.
116 The top common pathways identified include: cellular assembly and organization, cellular function and
117 maintenance, and cellular development and proliferation (**Supplementary Table 4**). The heatmaps in
118 **Figure 3** show the p value and the activation score for each pathway, and a graphical representation of the
119 cellular functions and genes involved, respectively. As shown in Figure 2, each gene expression FC is
120 proportional to their color intensity; orange arrows and pathways indicate a predicted activation, whereas
121 blue indicates increased levels of genes which lead to inhibition of the pathway. IPA analysis predicted an
122 activation of axonogenesis, axon branching, dendritic growth and branching and growth of neurites, based
123 on increased levels of genes such as VGF, FOS, PTGS2, JUN, BDNF, gamma-aminobutyric acid type A
124 receptor subunit beta3 (GABRB3), activating transcription factor 3 (ATF3), and cyclin dependent kinase
125 like 3 (CDKL3). We also found predicted activation of pathways regulating neuronal development, long-
126 term potentiation, and neurotransmission due to increased expression of genes such as FOS, PTGS2, EGR2,
127 BDNF, JUN, KCNJ2, ARC, and HOMER1.

128 Interestingly, we also found predicted inhibition of neuronal cell death, apoptosis and neuronal degeneration
129 pathways, together with increased survival of cerebral cortex cells, regeneration of axons, and cell viability,
130 due to increased expression of genes such as FOS, BDNF, ATF3, JUNB, DUSP1, neuronal PAS domain
131 protein 4 (NPAS4), nuclear factor interleukin 3 regulated (NFIL3), and SERPINE1.

132

133 **3) Comparison between contralateral and ipsilateral hemispheres**

134 Many studies utilize the contralateral neocortex as a convenient comparison tissue for DEG studies
135 (Volobueva et al. 2023), as SD does not directly propagate across the corpus collosum. However, even if
136 SD does not directly propagate through the contralateral cortex, the profound and widespread disruption of

137 neuronal network activity produced by SD might be expected to have some impact on neuronal activity and
138 gene expression in the contralateral hemisphere. The assumption that contralateral tissue is equivalent to
139 tissue from sham animals for DE analysis has not previously been tested.

140 We first performed DE analysis between these 2 tissues (i.e., contralateral hemispheres in animals exposed
141 to SD in the ipsilateral hemisphere vs. sham tissues). As showed in Supplementary Figure 2 no genes were
142 significant after FDR correction, confirming a high degree of similarity between gene expression in these
143 tissues.

144 We next performed the same analyses described above (**Figure 1**), but comparing tissue exposed to SD
145 with the contralateral cortex in the same animals, rather than shams. Of the 12893 mapped 33 significantly
146 upregulated after FDR correction (FDR <0.05) (**Figure 4A, red, FDR <0.05)**. IPA analysis confirmed a
147 high similarity between the sham and contralateral cortex when used as control compared to the SD group.
148 **Figure 4B** shows the top scored network (score 65) generated from the SD vs contralateral DEGs list and
149 the top diseases and function are reported in **Figure 4B** and **Supplementary Table 2 (compare with**
150 **Figure 2).** Likewise, **Figure 5** shows cellular and molecular pathways that are comparable with DEG
151 analysis with sham tissues (compared with Figure 3)**.** These results imply that, at least at the level of gene
152 expression changes at 2hours, the ipsilateral hemisphere that is not directly invaded by SD can likely serve
153 as an unaffected control.

154

155 **4) SD target genes control cell differentiation and proliferation, synaptic plasticity and stress**
156 **responses**

157 To validate the predicted activation of neuroprotective pathways, we analyzed the expression levels of
158 selected SD target genes by qRT-PCR. Based on the IPA results above, we focused on genes regulating 3
159 cellular functions: 1) cell differentiation and proliferation, 2) synaptic plasticity and 3) stress responses.
160 qPCR was performed on the same RNA that was subjected to the RNA-seq analyses, as well as 3 additional

161 animals for each group. As shown in **Figure 6**, multiple SDs resulted in significant increases in the
162 expression of genes activating cell proliferation and differentiation such as BNDF, DUPS6, FOS and JUNB
163 (**Figure 6**). Considering the predicted activation of neurons and long-term potentiation, as well the
164 increased axonogenesis, growth of neurites, and axon and neurites branching, we then analyzed the
165 expression of genes known for their regulation of synaptic plasticity. As shown in **Figure 6** we found
166 significantly increased expression of Homer1a and ARC. Finally, we examined levels of PTGS2, NR4A1,
167 and EGR2 as genes regulating stress and inflammatory responses.

168

169 **5) Target genes showed differential expression depending on the distance from the SD initiation site**

170 Lastly, we tested whether the levels of gene expression varied with distance from the SD initiation site. In
171 this set of studies, KCl was used as the stimulus, as the site of initiation is clearly restricted to small zone
172 of the application of KCl through the burrhole. Thus, two hours after onset of the initial SD, RNA was
173 extracted from either total contralateral cortex, or from 3 different regions of the ipsilateral hemisphere: 1)
174 SD initiation site; 2) intermediate site, and 3) remote site (see Methods and **Supplementary Figure 3**). By
175 qRT-PCR we analyzed the levels of the previously identified target genes (see section 3 above) and
176 compared these to the levels in the contralateral hemisphere of SHAM animals. For the majority of the
177 genes examined (BDNF, DUSP6, PTGS2 ARC, and Homer 1a), highest expression was detected in the
178 intermediate area (>3mm from the initiation site; **Figure 7**) while FOS and JUNB genes showed
179 significantly increased expression in the remote site (>6 mm from the initiation site). Interestingly, when
180 analyzing Homer1a levels, we found a decrease in their expression at the SD initiation site (**Figure 7**) when
181 compared to the contralateral and intermediate sites (**Figure 7**). The difference between the contralateral
182 and remote sites for NR4A1 did not reach statistical significance (p value=0.09) and EGR2 did not show
183 differential expression across regions (**Supplementary Figure 3**).

184

185 **Discussion**

186 As noted above (Introduction) previous work has identified molecular pathways linking SD to inflammation
187 and apoptosis, but there is interest in determining a wider spectrum of possible consequences of SD,
188 including possible contributions to plasticity and repair (Shuttleworth et al. 2020). Previous studies have
189 shown that SD leads to the increased synaptic activity (Sadowska et al. 2021; Kriz and Lalancette-Hébert
190 2009) as well as adult neurogenesis (Urbach et al. 2017; Urbach, Bruehl, and Witte 2006; Carmichael and
191 Chesselet 2002) and preconditioning (Matsushima et al. 1998; Yanamoto et al. 2004; Shen et al. 2016).
192 However, there has been limited investigation of specific molecular pathways underlying these processes.
193 Here, through RNA-seq and pathway analysis, we showed enrichment in genes regulating neurological
194 disorders, psychological disorders, and behavior (**Figure 2 and 4**). Furthermore, there were significant
195 increases in predicted pathways involving processes expected to be important for brain plasticity and repair,
196 including neuronal differentiation, and neurite growth and branching (**Figures 3 and 5**).
197

198 Prior exposure to SD has been shown to confer protection against subsequent ischemic challenges, and
199 increases in BDNF have previously been implicated in the mechanism (Matsushima et al. 1998; Yanamoto
200 et al. 2004). Consistent with previous work (Yanamoto et al. 2004; Rangel et al. 2001; Kokaia et al. 1993;
201 Matsushima et al. 1998), BDNF was one of the genes significantly increased by both KCl and optogenetic
202 stimuli (**Figure 6 and 7**) and was identified in SD-induced pathways related to neuronal differentiation
203 (**Figure 3 and 5**).
204 This study identified novel gene expression changes that could be used to test whether clusters of SD may
205 enhance plasticity. Importantly, the upregulation of SD specific target genes can lead to predicted inhibition
206 of pathways controlling neuronal cell death, apoptosis, and neuronal degeneration, together with increased
207 survival of cerebral cortex cells, regeneration of axons, and cell viability. The increased expression of genes
208 such as FOS, BDNF, JUNB, and neuronal PAS domain protein 4 (NPAS4), (**Figure 3 and 5),** lead to higher
209 rate of cellular development and differentiation compared to cell death and apoptosis. These genes have

210 been previously associated to increased neuronal tolerance for ischemic stroke (Yanamoto et al. 2004;
211 Matsushima et al. 1998; Takahashi et al. 2021).
212 Finally, we found increased expression of the mRNA for the plasticity-associated protein ARC, which
213 mediates AMPA receptors endocytosis and is required for protein synthesis dependent LTP and memory
214 formation (Chowdhury et al. 2006). Consistent with our findings, prior work in brain slices and rodent
215 cortex has reported LTP-like synaptic strengthening following SD (Footitt and Newberry 1998; Berger et
216 al. 2008), and it will be of interest to determine whether the time course of associated gene expression
217 changes correspond to variations in physiological recordings and how the expression of these genes change
218 under different metabolic conditions surrounding ischemic infarcts.
219
220 Although our results predict activation of neuroprotective pathways, they are also consistent with prior
221 reports of robust increases of the pro-inflammatory mediator COX2 (Takizawa et al. 2020; Kaido et al.
222 2012; Volobueva et al. 2023). We did not see significant increases in some other inflammatory mediators
223 (e.g., TNF-α, IL-1β, IL6), perhaps because the time course for peak increases in these mediators is later
224 than the 2-hour time point used in the present study (Takizawa et al. 2020). This time point was chosen
225 based on 1) prior expression analysis confirming peak increases at 2 hours for most genes of interest
226 (Kokaia et al. 1993; Karikó et al. 1998; Rangel et al. 2001) and 2) clinical recordings establishing clusters
227 of SDs (usually defined as three or more events within 2 hours) as being clinically significant (Hartings et
228 al. 2020; Dreier et al. 2006). Prior work (Takizawa et al. 2020) has shown that some inflammatory
229 mediators can be detected following a single SD (measured at 1 hour), while others peak at 24 h (Jander et
230 al. 2001; Matsushima et al. 1998; Volobueva et al. 2023). It remains to be determined which of the genes
231 seen here may peak earlier or at later times points.
232
233 To evaluate differences in gene expression at initiation sites vs. more remote sites, we micro-dissected
234 regions to compare differential expression of a number of key genes at the initiation, intermediate, and
235 remote sites using RT-qPCR analyses (**Figure 7 and Supplemental Figure 3**). We found that most genes

236 examined had largest increases at the intermediate site, >3 mm from the initiation site. If this is generally
237 true for other genes in the RNAseq data set, then it suggests that the initiation site with KCl stimulation
238 might not be a major contributor to DEG changes observed here. It is also possible that sites of SD initiation
239 and propagation could be different in SDs generated "spontaneously"/ naturalistically in patients or animal
240 models of migraine or brain injury. Thus, an SD initiation site required an area of coordinated
241 depolarization (Tang et al. 2014) from ischemia or synaptic stimulation with inadequate perfusion (von
242 Bornstädt et al. 2015). Gene expression changes in this environment may be quite different from changes
243 seen in remote areas into which the SD propagates. Spatial genomics approaches (Ibarra-Lopez et al. 2022)
244 will be useful to further investigate the distribution of changes of larger gene sets with distance from SD
245 initiation, and with respect to differential vascular perfusion, for example.
246
247 While most validated genes showed higher expression levels in the intermediate or remote sites and no
248 change in the initiation site, Homer1a showed a significant decrease in the SD initiation site (**Figure 7**).
249 Homer1 scaffolding protein controls the insertion of postsynaptic glutamate receptors (Ango et al. 2002;
250 Peng Luo et al. 2012). Homer1a is increased by synaptic activity through the MAP kinase pathway. This
251 type of regulation creates a negative feedback loop in which activity-dependent Homer1a inhibits
252 Homer1b/c ability to scaffold and diminishes synaptic strength by modulation of dendritic spine
253 morphology and AMPA/NMDA receptor activity (Bottai et al. 2002; Sato, Suzuki, and Nakanishi 2001).
254 This loop has been associated with TBI and epilepsy, particularly, and is thought to block postsynaptic
255 Ca^{2+}-mediated excitotoxicity (Cavarsan et al. 2012; P. Luo et al. 2014). Here, we found significantly
256 decreased levels of Homer1a in the initiation site, while expression was significantly increased in the
257 intermediate site. These results may suggest a negative feedback mechanism to reduce downstream
258 excitotoxicity, possibly reducing the number of glutamate postsynaptic receptors after repeated SDs.
259
260 **Conclusions**

261 Spreading depolarization (SD) is common in acute brain injury and contributes to expansion of lesions.
262 The potential role of SD in the recovery of surviving brain tissue is not yet clear. For the first time we
263 combined RNA-seq with predicted pathway analysis to identify a new range of molecular targets pathways
264 that could potentially be activated and contribute to circuit adaptation and recovery after brain **injury**
265 **(Figure 8)**. While it is very clear that SDs are direct contributors to injury in compromised brain tissue,
266 our findings suggest that multiple SDs could also activate a range of neuroprotective pathways including
267 increased cell proliferation, decreased cell death, cell differentiation, and neuronal plasticity (**Figure 2-5)**.
268 Whether or not such pathways make significant contributions to brain recovery and repair requires explicit
269 testing that can be guided, in part, by modification of key regulatory mediators identified in the present
270 study.
271
272

273 **Materials and Methods**

274 **Animal model**

275 All experimental procedures were performed in accordance with the National Institutes of Health Guide for
276 Care and Use of Laboratory Animals and were approved by the University of New Mexico Health Sciences
277 Center Institutional Animal Care and Use Committee (IACUC). SDs were induced repetitively (4 SDs in 2
278 hours at 30 min intervals) in healthy 7-8 week old female mice and SDs were confirmed with intrinsic
279 optical signal imaging (Supplementary Figure 1). SDs were induced in 6 mice with either focal application
280 of KCl through a burr hole in C57Bl6J mice (n=3) or with optogenetic stimulation (3 mW for 20 seconds)
281 in Thy1-ChR2-YFP positive mice (n=3). Thy1-ChR2-YFP breeders were initially purchased from The
282 Jackson Laboratory (B6.Cg-Tg(Thy1-COP4/EYFP)18Gfng/J, Strain #:007612,
283 RRID:IMSR_JAX:007612) and crossed to maintain the line, as previously described (Arenkiel et al. 2007).
284 With either stimulus, evoked SDs propagated throughout the neocortex ipsilateral to the stimulus, without
285 crossing to the contralateral hemisphere **(Supplementary Figure 1).** A matched number of sham controls

286 was used with focal NaCl administration through a burrhole, in C57Bl/6 mice (n=3), or 0.4 mW for 20
287 seconds in Thy1-ChR2-YFP positive mice (n=3). Thirty minutes after the last SD, the anesthetized animal
288 was decapitated and the brain extracted, washed with ice cold PBS and kept on ice.

289 **RNA extraction and qRT-PCR validation**

290 The contralateral and ipsilateral cortices were rapidly dissected from underlying striatum and the
291 hippocampus and total RNA was extracted using TRIzol (Invitrogen, ThermoFisher, Waltham, MA. USA).
292 Extractions were either from intact ipsilateral or contralateral cortices (**Figures 2-7**) or from regions ~18
293 mm^2 rapidly micro-dissected on ice (**Figure 7)**. Where indicated, microdissections were made from 3
294 different regions of the ipsilateral hemisphere: 1) SD initiation site; 2) intermediate site > 3mm from
295 initiation, 3) remote site >5 mm from initiation (**Supplementary Figure 3)**. All collected tissues were then
296 flash frozen and kept at –80°C until RNA extraction. RNA was quantified using Qubit (Bio-Rad) and its
297 quality was determined using a NanoDrop 1000 (ThermoFisher), using absorbance at 260, 280 and 230 nm.
298 Aliquots of 2 µg RNA were sent to Arraystar, Inc. for Illumina paired-end RNA-seq as described below.
299 To validate gene expression from our RNA-seq data set, separate aliquots containing 1 µg of total RNA
300 were reverse transcribed using SuperScript II reverse transcriptase (Life Technologies) following the
301 manufacturer's protocol and qPCR carried out with a CFX96 Touch Real-Time PCR Detection System
302 using SYBR Green mix (Life Technologies). Primer sequences for qRT-PCR for mouse mRNAs were
303 obtained from PrimerBank (https://pga.mgh.harvard.edu/primerbank/). The GAPDH gene (FW
304 TGTGATGGGTGTGAACCACGAGAA, RV GAGCCCTTCCACAATGCCAAAGTT) was used to
305 normalize values. As shown in **Supplementary Figure 3**, GAPDH expression itself was unchanged by SD
306 with either KCl or optogenetic induction of SD. The relative expression of target genes was determined
307 using the comparative 2−ΔCt method (Livak and Schmittgen 2001).

308 Values were expressed as means ± SEM. Statistical analysis was performed using GraphPad Prism version
309 9 (La Jolla, CA, USA). The data were analyzed by unpaired t-test followed by Welch's correction or

310 analysis of variance (ANOVA) followed by Dunnett's Multiple Comparison tests. Differences were
311 considered statistically significant when p values were < 0.05 (*p<0.05, **p<0.01, ***p<0.001).

312 **RNA-seq**

313 RNA sequencing analysis was performed by Arraystar Inc. (Rockville, MD). Total RNA (2 µg) was used
314 to prepare the sequencing library in the following steps: total RNA was enriched by oligo (dT) magnetic
315 beads (rRNA removed); RNA-seq library was prepared using KAPA Stranded RNA-Seq Library Prep Kit
316 (Illumina), which incorporates dUTP into the second cDNA strand and renders the RNA-seq library strand-
317 specific. The completed libraries were qualified with an Agilent 2100 Bioanalyzer and quantified by using
318 the absolute quantification qPCR method. To sequence the libraries on an Illumina NovaSeq 6000
319 instrument, the barcoded libraries were mixed, denatured to single stranded DNA in NaOH, captured on
320 Illumina flow cell, amplified *in situ,* and subsequently sequenced for 150 cycles for both ends on an Illumina
321 NovaSeq 6000 instrument. Sequence quality was examined using the FastQC software. The trimmed reads
322 (trimmed 5', 3'-adaptor bases using cutadapt) were aligned to a reference genome (Mouse genome
323 GRCm38) using Hisat2 software.

324 The data discussed in this publication have been deposited in NCBI's Gene Expression Omnibus (Edgar,
325 Domrachev, and Lash 2002) and are accessible through GEO Series accession number GSE214623
326 (https://www.ncbi.nlm.nih.gov/geo/query/acc.cgi?acc=GSE214623).

327 **Differential expression analysis**

328 The expression levels of known genes and transcripts were calculated using the StringTie and Ballgown
329 software package (Pertea et al. 2016) and expressed as fragments per kilobase of transcript per million
330 mapped reads (FPKM). Only genes with minimal counts per million (CPM) in at least one library were kept
331 for further analysis. Differentially expressed gene (DEG) and transcript analyses were performed using an
332 unpaired t-test followed by Welch's correction; a fold change (FC) threshold of 1.25 and p value < 0.05

333 were used together to classify genes and transcripts as differentially expressed. We subsequently performed
334 DESeq2 analysis (Ge, Son, and Yao 2018) with a false discovery rate (FDR) correction cutoff of 0.05.

335 **Ingenuity Pathway Analysis**

336 Predicted molecular functions and biological pathways enriched in genes differentially expressed after SD
337 were identified using Ingenuity Pathway software (IPA, Content version: 62089861 (Release Date: 2021-
338 02-17), Qiagen, https://www.qiagenbioinformatics.com/products/ingenuity-pathway-analysis). The
339 analysis was set to filter nervous system expressed genes only; reference set: Ingenuity Knowledge Base
340 (Genes Only); and including direct and indirect relationships.

341

342 **Acknowledgments:** We thank the Animal Research Facility (ARF) of the Health Science Center (HSC),
343 University of New Mexico School of Medicine. We also thank the UNM Preclinical Core of the Center
344 from Brain Recovery and Repair (University of New Mexico) for technical support.

345 **Funding:** This work was supported by the National Institute of Health grants NS106901 and
346 P206GM109089.

347

348

349

350

351 **References**

352 Aiba, Isamu, Andrew P. Carlson, Christian T. Sheline, and Shuttleworth C. William. 2012. "Synaptic
353 Release and Extracellular Actions of Zn 2+ Limit Propagation of Spreading Depression and Related
354 Events in Vitro and in Vivo." *Journal of Neurophysiology* 107 (3): 1032–41.

355 https://doi.org/10.1152/jn.00453.2011.

356 Ango, Fabrice, David Robbe, Jian Cheng Tu, Bo Xiao, Paul F Worley, Jean-Philippe Pin, Joël Bockaert,
357 and Laurent Fagni. 2002. "Homer-Dependent Cell Surface Expression of Metabotropic Glutamate
358 Receptor Type 5 in Neurons." *Molecular and Cellular Neurosciences* 20 (2): 323–29.
359 http://www.ncbi.nlm.nih.gov/pubmed/12093163.

360 Arenkiel, Benjamin R., Joao Peca, Ian G. Davison, Catia Feliciano, Karl Deisseroth, George J J.
361 Augustine, Michael D. Ehlers, and Guoping Feng. 2007. "In Vivo Light-Induced Activation of
362 Neural Circuitry in Transgenic Mice Expressing Channelrhodopsin-2." *Neuron* 54 (2): 205–18.
363 https://doi.org/10.1016/J.NEURON.2007.03.005.

364 Ayata, Cenk, and Martin Lauritzen. 2015. "Spreading Depression, Spreading Depolarizations, and the
365 Cerebral Vasculature." *Physiological Reviews* 95 (3): 953–93.
366 https://doi.org/10.1152/PHYSREV.00027.2014.

367 Berger, M., E. J. Speckmann, H. C. Pape, and A. Gorji. 2008. "Spreading Depression Enhances Human
368 Neocortical Excitability in Vitro." *Cephalalgia : An International Journal of Headache* 28 (5): 558–
369 62. https://doi.org/10.1111/J.1468-2982.2008.01556.X.

370 Bornstädt, Daniel von, Thijs Houben, Jessica L. Seidel, Yi Zheng, Ergin Dilekoz, Tao Qin, Nora Sandow,
371 et al. 2015. "Supply-Demand Mismatch Transients in Susceptible Peri-Infarct Hot Zones Explain
372 the Origins of Spreading Injury Depolarizations." *Neuron* 85 (5): 1117–31.
373 https://doi.org/10.1016/J.NEURON.2015.02.007.

374 Bottai, Daniele, John F. Guzowski, Martin K. Schwarz, Shin H. Kang, Bo Xiao, Anthony Lanahan, Paul
375 F. Worley, and Peter H. Seeburg. 2002. "Synaptic Activity-Induced Conversion of Intronic to
376 Exonic Sequence in Homer 1 Immediate Early Gene Expression." *The Journal of Neuroscience* 22
377 (1): 167. https://doi.org/10.1523/JNEUROSCI.22-01-00167.2002.

Carlson, Andrew P., Mohammad Abbas, Robert L. Alunday, Fares Qeadan, and C. William Shuttleworth. 2018. "Spreading Depolarization in Acute Brain Injury Inhibited by Ketamine: A Prospective, Randomized, Multiple Crossover Trial." *Journal of Neurosurgery* 130 (5): 1513–19. https://doi.org/10.3171/2017.12.JNS171665.

Carmichael, S. Thomas, and Marie Françoise Chesselet. 2002. "Synchronous Neuronal Activity Is a Signal for Axonal Sprouting after Cortical Lesions in the Adult." *Journal of Neuroscience* 22 (14): 6062–70. https://doi.org/10.1523/JNEUROSCI.22-14-06062.2002.

Cavarsan, C. F., F. Tescarollo, C. Tesone-Coelho, R. L.T. Morais, F. L.T. Motta, M. M. Blanco, and L. E. Mello. 2012. "Pilocarpine-Induced Status Epilepticus Increases Homer1a and Changes MGluR5 Expression." *Epilepsy Research* 101 (3): 253–60. https://doi.org/10.1016/J.EPLEPSYRES.2012.04.011.

Charles, A., and K. C. Brennan. 2009. "Cortical Spreading Depression-New Insights and Persistent Questions." *Cephalalgia : An International Journal of Headache* 29 (10): 1115–24. https://doi.org/10.1111/J.1468-2982.2009.01983.X.

Chowdhury, Shoaib, Jason D. Shepherd, Hiroyuki Okuno, Gregory Lyford, Ronald S. Petralia, Niels Plath, Dietmar Kuhl, Richard L. Huganir, and Paul F. Worley. 2006. "Arc Interacts with the Endocytic Machinery to Regulate AMPA Receptor Trafficking." *Neuron* 52 (3): 445. https://doi.org/10.1016/J.NEURON.2006.08.033.

Dietrich, W D, J Truettner, R Prado, N E Stagliano, W Zhao, R Busto, M D Ginsberg, and B D Watson. 2000. "Thromboembolic Events Lead to Cortical Spreading Depression and Expression of C-Fos, Brain-Derived Neurotrophic Factor, Glial Fibrillary Acidic Protein, and Heat Shock Protein 70 MRNA in Rats." *Journal of Cerebral Blood Flow and Metabolism : Official Journal of the International Society of Cerebral Blood Flow and Metabolism* 20 (1): 103–11. https://doi.org/10.1097/00004647-200001000-00014.

402 Dreier, Jens P. 2011. “The Role of Spreading Depression, Spreading Depolarization and Spreading
403 Ischemia in Neurological Disease.” *Nature Medicine* 17 (4): 439–47.
404 https://doi.org/10.1038/nm.2333.

405 Dreier, Jens P., Martin Fabricius, Cenk Ayata, Oliver W. Sakowitz, C. William Shuttleworth, Christian
406 Dohmen, Rudolf Graf, et al. 2017. “Recording, Analysis, and Interpretation of Spreading
407 Depolarizations in Neurointensive Care: Review and Recommendations of the COSBID Research
408 Group.” *Journal of Cerebral Blood Flow and Metabolism* 37 (5): 1595–1625.
409 https://doi.org/10.1177/0271678X16654496.

410 Dreier, Jens P., Johannes Woitzik, Martin Fabricius, Robin Bhatia, Sebastian Major, Chistoph
411 Drenckhahn, Thomas Nicolas Lehmann, et al. 2006. “Delayed Ischaemic Neurological Deficits after
412 Subarachnoid Haemorrhage Are Associated with Clusters of Spreading Depolarizations.” *Brain : A*
413 *Journal of Neurology* 129 (Pt 12): 3224–37. https://doi.org/10.1093/BRAIN/AWL297.

414 Edgar, Ron, Michael Domrachev, and Alex E. Lash. 2002. “Gene Expression Omnibus: NCBI Gene
415 Expression and Hybridization Array Data Repository.” *Nucleic Acids Research* 30 (1): 207–10.
416 https://doi.org/10.1093/NAR/30.1.207.

417 Eising, Else, Reinald Shyti, Peter A.C. ’t Hoen, Lisanne S. Vijfhuizen, Sjoerd M.H. Huisman, Ludo A.M.
418 Broos, Ahmed Mahfouz, et al. 2017. “Cortical Spreading Depression Causes Unique Dysregulation
419 of Inflammatory Pathways in a Transgenic Mouse Model of Migraine.” *Molecular Neurobiology* 54
420 (4): 2986–96. https://doi.org/10.1007/S12035-015-9681-5.

421 Footitt, David R., and Nigel R. Newberry. 1998. “Cortical Spreading Depression Induces an LTP-like
422 Effect in Rat Neocortex in Vitro.” *Brain Research* 781 (1–2): 339–42.
423 https://doi.org/10.1016/S0006-8993(97)01359-0.

424 García-Campos, Miguel A., Jesús Espinal-Enríquez, and Enrique Hernández-Lemus. 2015. “Pathway
425 Analysis: State of the Art.” *Frontiers in Physiology* 6 (DEC): 383.

426 https://doi.org/10.3389/FPHYS.2015.00383/BIBTEX.

427 Ge, Steven Xijin, Eun Wo Son, and Runan Yao. 2018. "IDEP: An Integrated Web Application for
428 Differential Expression and Pathway Analysis of RNA-Seq Data." *BMC Bioinformatics* 19 (1): 1–
429 24. https://doi.org/10.1186/s12859-018-2486-6.

430 Hartings, Jed A., Norberto Andaluz, M. Ross Bullock, Jason M. Hinzman, Bruce Mathern, Clemens Pahl,
431 Ava Puccio, et al. 2020. "Prognostic Value of Spreading Depolarizations in Patients With Severe
432 Traumatic Brain Injury." *JAMA Neurology* 77 (4): 489–99.
433 https://doi.org/10.1001/JAMANEUROL.2019.4476.

434 Hartings, Jed A., C. William Shuttleworth, Sergei A. Kirov, Cenk Ayata, Jason M. Hinzman, Brandon
435 Foreman, R. David Andrew, et al. 2017. "The Continuum of Spreading Depolarizations in Acute
436 Cortical Lesion Development: Examining Leão's Legacy." *Journal of Cerebral Blood Flow and*
437 *Metabolism* 37 (5): 1571–94. https://doi.org/10.1177/0271678X16654495.

438 Helbok, Raimund, Jed A. Hartings, Alois Schiefecker, Baptiste Balança, Sharon Jewel, Brandon
439 Foreman, Ari Ercole, et al. 2020. "What Should a Clinician Do When Spreading Depolarizations
440 Are Observed in a Patient?" *Neurocritical Care* 32 (1): 306–10. https://doi.org/10.1007/s12028-019-
441 00777-6.

442 Hinzman, Jason M., Vince A. DiNapoli, Eric J. Mahoney, Greg A. Gerhardt, and Jed A. Hartings. 2015.
443 "Spreading Depolarizations Mediate Excitotoxicity in the Development of Acute Cortical Lesions."
444 *Experimental Neurology* 267 (May): 243–53. https://doi.org/10.1016/j.expneurol.2015.03.014.

445 Ibarra-Lopez, Veronica, Sangeeta Jayakar, Yeqing Angela Yang, Ciara Martin, Zora Modrusan, and
446 Sandra Rost. 2022. "Spatial Profiling of Protein and RNA Expression in Tissue: An Approach to
447 Fine-Tune Virtual Microdissection." *Journal of Visualized Experiments : JoVE*, no. 185 (July).
448 https://doi.org/10.3791/62651.

449 Jander, S, M Schroeter, O Peters, O W Witte, and G Stoll. 2001. "Cortical Spreading Depression Induces
450 Proinflammatory Cytokine Gene Expression in the Rat Brain." *J. Cereb. Blood Flow Metab.* 21 (3):
451 218–25. https://doi.org/10.1097/00004647-200103000-00005.

452 Kaido, Kempski, Heimann, Heers, and Bartsch. 2012. "Cluster Analysis of MRNA Expression Levels
453 Identifies Multiple Sequential Patterns Following Focal Cerebral Ischemia." *Turkish Neurosurgery*
454 22 (4). https://doi.org/10.5137/1019-5149.JTN.5523-11.0.

455 Karikó, Katalin, Valerie A. Harris, Yolanda Rangel, Monica E. Duvall, and Frank A. Welsh. 1998.
456 "Effect of Cortical Spreading Depression on the Levels of MRNA Coding for Putative
457 Neuroprotective Proteins in Rat Brain." *Journal of Cerebral Blood Flow and Metabolism* 18 (12):
458 1308–15. https://doi.org/10.1097/00004647-199812000-00005.

459 Kokaia, Zaal, Gunilla Gidö, Tomas Ringstedt, Johan Bengzon, Merab Kokaia, Bo K. Siesjö, Håkan
460 Persson, and Olle Lindvall. 1993. "Rapid Increase of BDNF MRNA Levels in Cortical Neurons
461 Following Spreading Depression: Regulation by Glutamatergic Mechanisms Independent of Seizure
462 Activity." *Molecular Brain Research* 19 (4): 277–86. https://doi.org/10.1016/0169-328X(93)90126-
463 A.

464 Kriz, Jasna, and Mélanie Lalancette-Hébert. 2009. "Inflammation, Plasticity and Real-Time Imaging after
465 Cerebral Ischemia." *Acta Neuropathologica* 117 (5): 497–509. https://doi.org/10.1007/S00401-009-
466 0496-1.

467 Lauritzen, Martin, Jens Peter Dreier, Martin Fabricius, Jed A. Hartings, Rudolf Graf, and Anthony John
468 Strong. 2011. "Clinical Relevance of Cortical Spreading Depression in Neurological Disorders:
469 Migraine, Malignant Stroke, Subarachnoid and Intracranial Hemorrhage, and Traumatic Brain
470 Injury." *Journal of Cerebral Blood Flow and Metabolism* 31 (1): 17–35.
471 https://doi.org/10.1038/jcbfm.2010.191.

472 Leao, Aristides A. P. 1944. "SPREADING DEPRESSION OF ACTIVITY IN THE CEREBRAL

473 CORTEX." *Journal of Neurophysiology* 7 (6): 359–90. https://doi.org/10.1152/jn.1944.7.6.359.

474 Lindquist, Britta E., and C. William Shuttleworth. 2014. "Spreading Depolarization-Induced Adenosine
475 Accumulation Reflects Metabolic Status in Vitro and in Vivo." *Journal of Cerebral Blood Flow and*
476 *Metabolism* 34 (11): 1779–90. https://doi.org/10.1038/jcbfm.2014.146.

477 Livak, Kenneth J., and Thomas D. Schmittgen. 2001. "Analysis of Relative Gene Expression Data Using
478 Real-Time Quantitative PCR and the 2-ΔΔCT Method." *Methods* 25 (4): 402–8.
479 https://doi.org/10.1006/meth.2001.1262.

480 Luo, P., T. Chen, Y. Zhao, L. Zhang, Y. Yang, W. Liu, S. Li, et al. 2014. "Postsynaptic Scaffold Protein
481 Homer 1a Protects against Traumatic Brain Injury via Regulating Group I Metabotropic Glutamate
482 Receptors." *Cell Death & Disease* 5 (4). https://doi.org/10.1038/CDDIS.2014.116.

483 Luo, Peng, Xia Li, Zhou Fei, and Waisang Poon. 2012. "Scaffold Protein Homer 1: Implications for
484 Neurological Diseases." *Neurochemistry International* 61 (5): 731–38.
485 https://doi.org/10.1016/j.neuint.2012.06.014.

486 Matsushima, Kazushi, Matthew J Hogan, and Antoine M Hakim. 1996. "Cortical Spreading Depression
487 Protects against Subsequent Focal Cerebral Ischemia in Rats." *J. Cereb. Blood Flow Metab.* 16 (2):
488 221–26. https://doi.org/10.1097/00004647-199603000-00006.

489 Matsushima, Kazushi, Rainald Schmidt-Kastner, Matthew J. Hogan, and Antoine M. Hakim. 1998.
490 "Cortical Spreading Depression Activates Trophic Factor Expression in Neurons and Astrocytes and
491 Protects against Subsequent Focal Brain Ischemia." *Brain Res.* 807 (1,2): 47–60.
492 https://doi.org/10.1016/s0006-8993(98)00716-1.

493 Nedergaard, Maiken, and Anker Jon Hansen. 1988. "Spreading Depression Is Not Associated with
494 Neuronal Injury in the Normal Brain." *Brain Research* 449 (1–2): 395–98.
495 https://doi.org/10.1016/0006-8993(88)91062-1.

496 Pertea, Mihaela, Daehwan Kim, Geo M. Pertea, Jeffrey T. Leek, and Steven L. Salzberg. 2016.
497 "Transcript-Level Expression Analysis of RNA-Seq Experiments with HISAT, StringTie and
498 Ballgown." *Nature Protocols 2016 11:9* 11 (9): 1650–67. https://doi.org/10.1038/nprot.2016.095.

499 Pietrobon, Daniela, and Michael A. Moskowitz. 2014. "Chaos and Commotion in the Wake of Cortical
500 Spreading Depression and Spreading Depolarizations." *Nature Reviews. Neuroscience* 15 (6): 379–
501 93. https://doi.org/10.1038/NRN3770.

502 Rangel, Yolanda M., Katalin Karikó, Valerie A. Harris, Monica E. Duvall, and Frank A. Welsh. 2001.
503 "Dose-Dependent Induction of MRNAs Encoding Brain-Derived Neurotrophic Factor and Heat-
504 Shock Protein-72 after Cortical Spreading Depression in the Rat." *Molecular Brain Research* 88 (1–
505 2): 103–12. https://doi.org/10.1016/S0169-328X(01)00037-7.

506 Sadowska, M, Mehlhorn C, Średniawa W, Szewczyk ŁM, Szlachcic A, Urban P, Winiarski M, and
507 Jabłonka JA. 2021. "Spreading Depressions and Periinfarct Spreading Depolarizations in the
508 Context of Cortical Plasticity." *Neuroscience* 453 (January): 81–101.
509 https://doi.org/10.1016/J.NEUROSCIENCE.2020.10.032.

510 Sato, Masaaki, Kazunori Suzuki, and Shigetada Nakanishi. 2001. "NMDA Receptor Stimulation and
511 Brain-Derived Neurotrophic Factor Upregulate Homer 1a MRNA via the Mitogen-Activated Protein
512 Kinase Cascade in Cultured Cerebellar Granule Cells." *The Journal of Neuroscience : The Official*
513 *Journal of the Society for Neuroscience* 21 (11): 3797–3805.
514 https://doi.org/10.1523/JNEUROSCI.21-11-03797.2001.

515 Shen, Ping Ping, Shuai Hou, Di Ma, Ming Ming Zhao, Ming Qin Zhu, Jing Dian Zhang, Liang Shu Feng,
516 Li Cui, and Jia Chun Feng. 2016. "Cortical Spreading Depression-Induced Preconditioning in the
517 Brain." *Neural Regeneration Research* 11 (11): 1857–64. https://doi.org/10.4103/1673-
518 5374.194759.

519 Shuttleworth, C. William, R. David Andrew, Yama Akbari, Cenk Ayata, Ramani Balu, K. C. Brennan,

520 Martyn Boutelle, et al. 2020. “Which Spreading Depolarizations Are Deleterious To Brain Tissue?”
521 *Neurocritical Care* 32 (1): 317–22. https://doi.org/10.1007/s12028-019-00776-7.

522 Sintas, Cèlia, Noèlia Fernàndez-Castillo, Marta Vila-Pueyo, Patricia Pozo-Rosich, Alfons Macaya, and
523 Bru Cormand. 2017. “Transcriptomic Changes in Rat Cortex and Brainstem After Cortical
524 Spreading Depression With or Without Pretreatment With Migraine Prophylactic Drugs.” *The*
525 *Journal of Pain* 18 (4): 366–75. https://doi.org/10.1016/j.jpain.2016.11.007.

526 Takizawa, Tsubasa, Tao Qin, Andreia Lopes de Morais, Kazutaka Sugimoto, Joon Yong Chung, Liza
527 Morsett, Inge Mulder, et al. 2020. “Non-Invasively Triggered Spreading Depolarizations Induce a
528 rapidpro-Inflammatory Response in Cerebral Cortex.” *Journal of Cerebral Blood Flow &*
529 *Metabolism* 40 (5): 1117. https://doi.org/10.1177/0271678X19859381.

530 Tang, Yujie T., Jorge M. Mendez, Jeremy J. Theriot, Punam M. Sawant, Héctor E. López-Valdés, Y.
531 Sungtaek Ju, and K. C. Brennan. 2014. “Minimum Conditions for the Induction of Cortical
532 Spreading Depression in Brain Slices.” *Journal of Neurophysiology* 112 (10): 2572–79.
533 https://doi.org/10.1152/JN.00205.2014.

534 Urbach, Anja, Eileen Baum, Falko Braun, and Otto W. Witte. 2017. “Cortical Spreading Depolarization
535 Increases Adult Neurogenesis, and Alters Behavior and Hippocampus-Dependent Memory in
536 Mice.” *Journal of Cerebral Blood Flow and Metabolism* 37 (5): 1776–90.
537 https://doi.org/10.1177/0271678X16643736.

538 Urbach, Anja, Claus Bruehl, and Otto W. Witte. 2006. “Microarray-Based Long-Term Detection of
539 Genes Differentially Expressed after Cortical Spreading Depression.” *European Journal of*
540 *Neuroscience* 24 (3): 841–56. https://doi.org/10.1111/j.1460-9568.2006.04862.x.

541 Volobueva, Maria N., Elena M. Suleymanova, Maria P. Smirnova, Alexey P. Bolshakov, and Lyudmila
542 V. Vinogradova. 2023. “A Single Episode of Cortical Spreading Depolarization Increases MRNA
543 Levels of Proinflammatory Cytokines, Calcitonin Gene-Related Peptide and Pannexin-1 Channels in

544 the Cerebral Cortex." *International Journal of Molecular Sciences* 24 (1).
545 https://doi.org/10.3390/ijms24010085.

546 Yanamoto, Hiroji, Jing Hui Xue, Susumu Miyamoto, Izumi Nagata, Yoshikazu Nakano, Kenichi Murao,
547 and Haruhiko Kikuchi. 2004. "Spreading Depression Induces Long-Lasting Brain Protection against
548 Infarcted Lesion Development via BDNF Gene-Dependent Mechanism." *Brain Res.* 1019 (1,2):
549 178–88. https://doi.org/10.1016/j.brainres.2004.05.105.

550

551

552 **Figure Legends**

553 **Figure 1. Differential Expression (DE) analysis.** We performed unpaired t-test followed by Welch's
554 correction; significant genes (FC > 1.25, p value <0.05) are represented in black. Consequently, we
555 performed DESeq2 analysis (Ge, Son, and Yao 2018); genes that were also significant after False Rate
556 Discovery correction (FDR <0.05) are represented in red.

557

558 **Figure 2. A) and B) top Molecular networks (score 63 and 32) generated by IPA analysis of DEGs**
559 **upregulated in SD animals vs Sham.** The intensity of the color red for each molecule is proportional to
560 the FC of the gene. Full arrows indicate a direct relationship between molecules, while dotted arrows
561 indicate an indirect relationship between genes. Orange arrows indicate the predicted activation of a gene,
562 while yellow indicates predicted inhibition. **C) Top Diseases and Functions.**

563

564 **Figure 3. Top Cellular functions generated by IPA analysis of DEGs upregulated in SD animals vs**
565 **Sham.** Top pathways identified include: cellular assembly and organization, cellular function and
566 maintenance, and cellular development and proliferation**.** The heatmaps show the p value and the activation
567 score for each pathway, and a graphical representation of the networks and the genes respectively involved.
568 In particular, the intensity of the color red for each molecule is proportional to the FC of the gene. Orange
569 arrows indicate a positive control of the gene on the related pathway, and the pathway's name highlighted
570 in orange indicates its activation.

571

572 **Figure 4. A) Differential Expression (DE) analysis.** We performed unpaired t-test followed by Welch's
573 correction; significant genes (FC > 1.25, p value <0.05) are represented in black. Consequently, we

574 performed DESeq2 analysis (Ge, Son, and Yao 2018); genes that were also significant after False Rate
575 Discovery correction (FDR <0.05) are represented in red, in green we highlighted the genes in common
576 with SD vs Sham DE analysis. **B) top molecular network (score 65) generated by IPA analysis of DEGs**
577 **upregulated in SD animals vs Contralateral.** The intensity of the color red for each molecule is
578 proportional to the FC of the gene. Full arrows indicate a direct relationship between molecules, while
579 dotted arrows indicate an indirect relationship between genes. Orange arrows indicate the predicted
580 activation of a gene, while yellow indicates predicted inhibition. **C) Top Diseases and Functions.**

581

582 **Figure 5. Top Cellular functions generated by IPA analysis of DEGs upregulated in SD animals vs**
583 **Contralateral.** Top pathways identified include: cellular assembly and organization, cellular function and
584 maintenance, and cellular development and proliferation**.** The heatmaps show the p value and the activation
585 score for each pathway, and a graphical representation of the networks and the genes respectively involved.
586 In particular, the intensity of the color red for each molecule is proportional to the FC of the gene. Orange
587 arrows indicate a positive control of the gene on the related pathway, and the pathway's name highlighted
588 in orange indicates its activation.

589

590 **Figure 6. RT-qPCR validation of SD target genes identified by RNA-seq.** mRNA levels of the target
591 genes were measured as described in Material and Methods. Data were analyzed by unpaired t-test,
592 followed by Welch's correction and are represented as mean ± SEM; $p<0.05$*, **$p<0.01$, ***$p<0.001$; n=6.

593

594 **Figure 7. Target genes showed differential expression depending on the distance from the SD**
595 **initiation site.** mRNA levels of the target genes were measured as described in Material and Methods.
596 Specifically, we determined the mRNA levels in 4 different regions: 1) SD initiation site, 2) SD intermediate
597 site, 3) SD remote site, and 4) the contralateral hemisphere. Data were analyzed by 2-way ANOVA

598 followed by Tukey's Multiple Comparison test, and are represented as mean ± SEM; $p<0.05$*, **$p<0.01$,
599 ***$p<0.001$; and unpaired t-test, followed by Welch's correction and are represented as mean ± SEM;
600 $^{\#}p<0.05$, $^{\#\#}p<0.01$, $^{\#\#\#}p<0.001$; n=3.

601

602 **Figure 8.** The combination of unbiased RNA-seq analysis with predicted pathway analysis showed that
603 clusters of SDs could activate a range of neuroprotective pathways including increased cell proliferation,
604 decreased cell death, cell differentiation, and neuronal plasticity. The identification of molecular markers
605 responsible for the activation of this pathways could lead to the discovery of new therapeutic targets.

606

607 **Supplementary Figure 1. Schematic representation of the SDs induction:** SDs were induced
608 repetitively (4 SDs in 2 hours at 30 min intervals) in healthy, female mice and SDs were confirmed with
609 Intrinsic Optical Signal imaging. SD induction was with either focal application of KCl (NaCl for sham
610 controls, n=6) in C57Bl/6 mice or with optogenetic stimulation (2 mW for 20 seconds) in Thy1-ChR2-YFP
611 mice (n=6). **C) iOS images of the SDs propagating through the left hemisphere**; after KCl application,
612 or Optogenetic stimulation.

613

614 **Supplementary Figure 2 Differential Expression (DE) analysis.** We performed unpaired t-test followed
615 by Welch's correction; significant genes (FC > 1.25, p value <0.05) are represented in black. Consequently,
616 we performed DESeq2 analysis (Ge, Son, and Yao 2018); no genes significant after False Rate Discovery
617 correction (FDR <0.1).

618

619 **Supplementary Figure 3. A)** Representation of the localization of the micro dissected tissues collected for
620 qRT-PCR **B)** GAPDH levels in RNA sequencing samples are expressed as FPKM. No differences in

621 GAPDH were found after either KCl- or optogenetic- induced SDs. Thus, GAPDH represents a valid hkg
622 for qRT-PCR validation. Data were analyzed by unpaired t-test, followed by Welch's correction and
623 represented as mean ± SEM, n=3. **C)** Target genes showed differential expression depending on the distance
624 from the SD initiation site. mRNA levels of the target genes were measured as described in Material and
625 Methods. Specifically, we determined the mRNA levels in 4 different regions: 1) SD initiation site, 2) SD
626 intermediate site, 3) SD remote site, and 4) the contralateral hemisphere. Data were analyzed by 2-way
627 ANOVA followed by Tukey's Multiple Comparison test, and are represented as mean ± SEM; n=3.

628

629

630

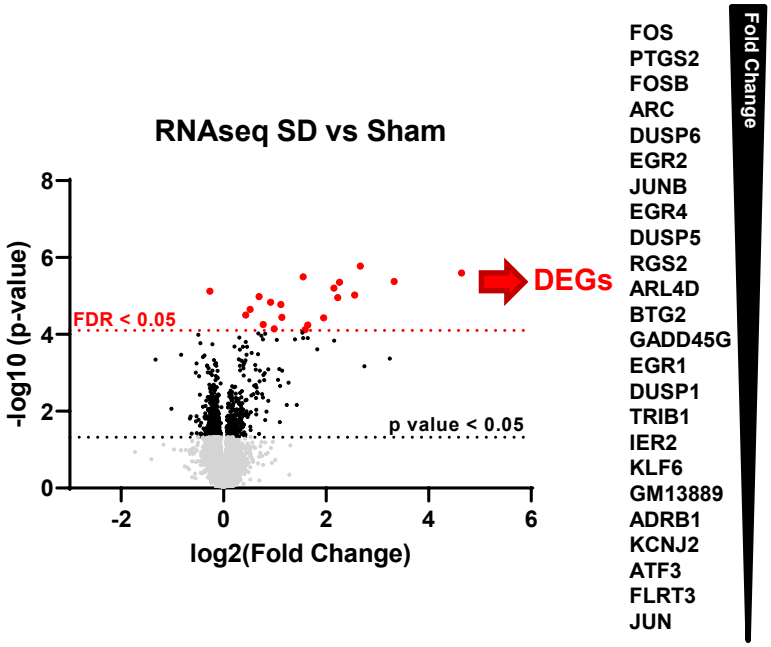
RNAseq SD vs Sham
-log10 (p-value)
log2(Fold Change)
FDR < 0.05
p value < 0.05
DEGs
8
6
4
2
0
-2
0
2
4
6
FOS
PTGS2
FOSB
ARC
DUSP6
EGR2
JUNB
EGR4
DUSP5
RGS2
ARL4D
BTG2
GADD45G
EGR1
DUSP1
TRIB1
IER2
KLF6
GM13889
ADRB1
KCNJ2
ATF3
FLRT3
JUN
Fold Change

2A.

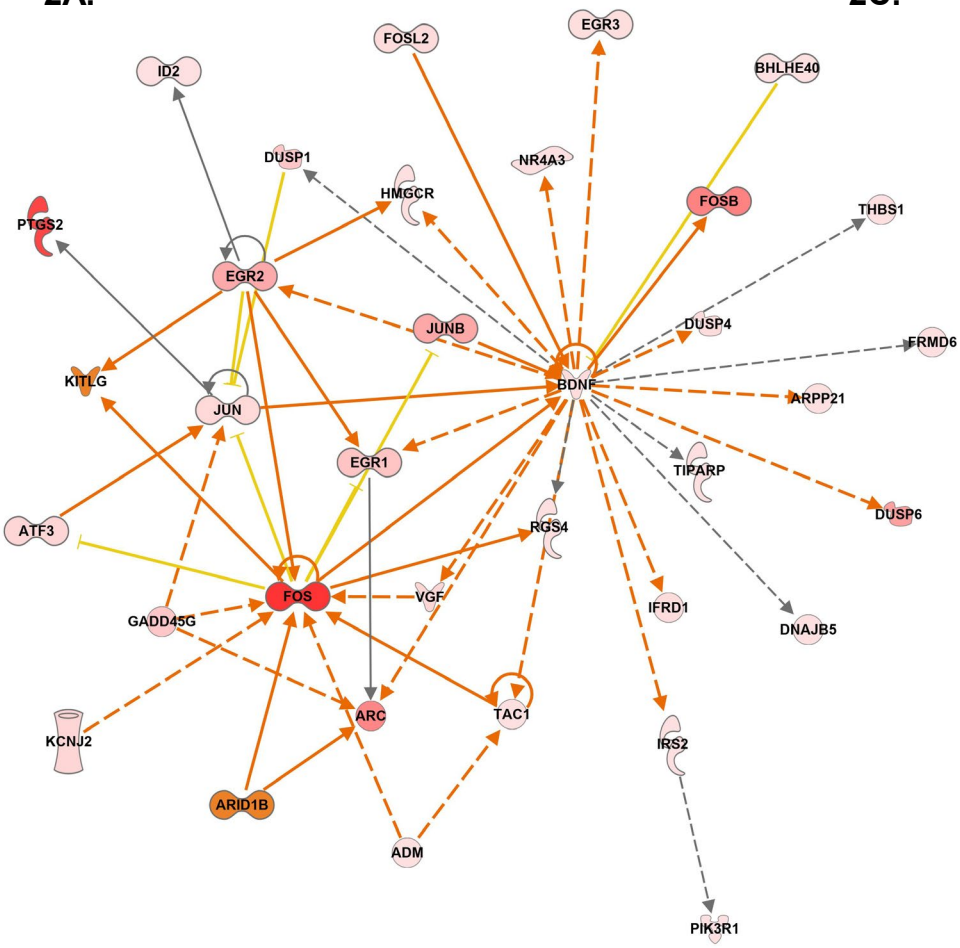

2C.

Disease and Disorders	p-value range	# Molecules
Neurological Diseases	3.69E-02 - 7.77E-09	42
Organismal Injury and Abnormalities	3.69E-02 - 6.10E-09	43
Psychological Disorders	2.65E-02 - 6.10E-09	29
Hereditary Disorders	2.65E-02 - 6.10E-09	18
Skeletal and Muscular Disorders	2.65E-02 - 2.70E-08	17

Physiological System Development and Functions	p-value range	# Molecules
Nervous System Development and Function	3.69E-02 - 7.62E-07	51
Tissue Morphology	3.69E-02 - 4.54E-08	28
Tissue Development	3.46E-02 - 7.62E-07	40
Organismal Development	3.46E-02 - 4.43E-06	37
Behavior	3.17E-02 - 1.11E-05	12

2B.

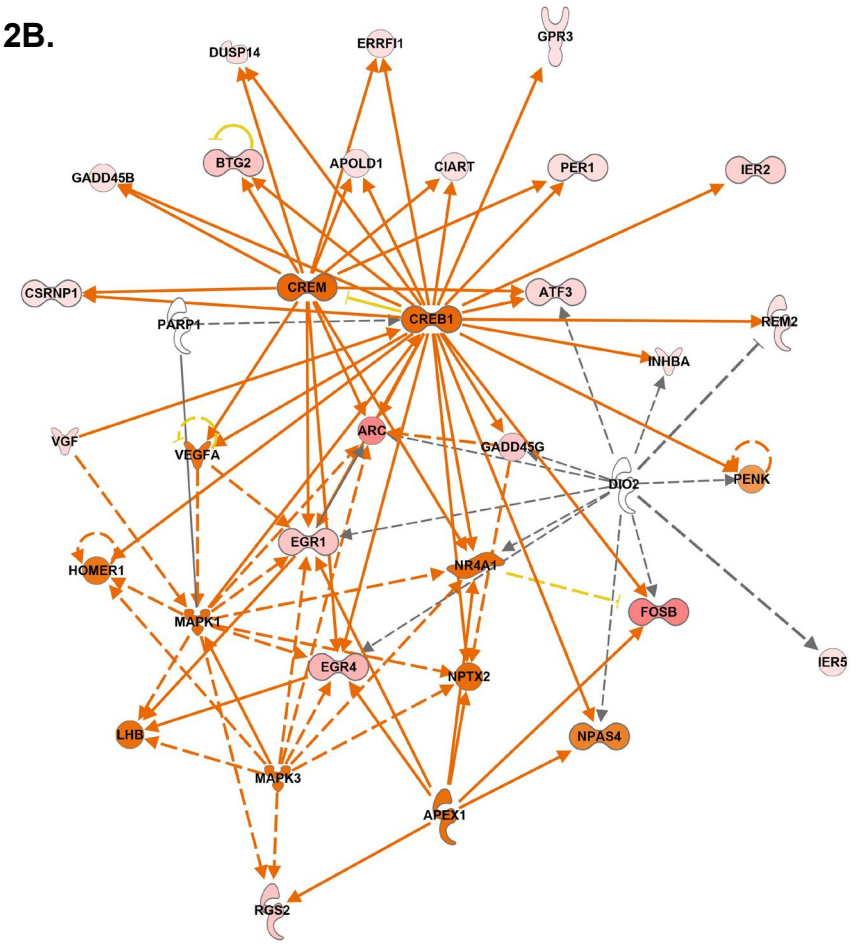

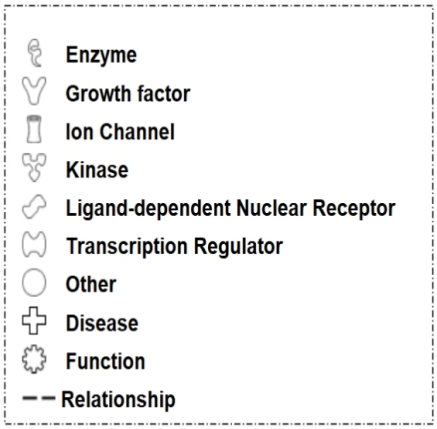

	p-value	Activation Score
Cell death of hippocampal neurons	8.02E-05	-2.410
Apoptosis	4.95E-07	-2.003
Neuronal cell death	1.68E-05	-1.974
Cell death of cerebral cortex cells	0.000146	-1.589
Degeneration of neurons	0.0309	-0.660
Cell death of neuroglia	0.00234	-0.339
Cell death of cortical neurons	0.033	-0.283
Apoptosis of granule cells	6.06E-05	-0.266
Apoptosis of neuroglia	0.00413	-0.152
Apoptosis of sympathetic neuron	0.000254	-0.145
Cell viability of hippocampal neurons	0.00023	1.124
Cell viability of cerebral cortex cells	0.000519	1.413
Survival of cephalic neurons	0.000519	1.413
Survival of neural cells	0.0241	1.774
Cell viability	0.0263	1.774

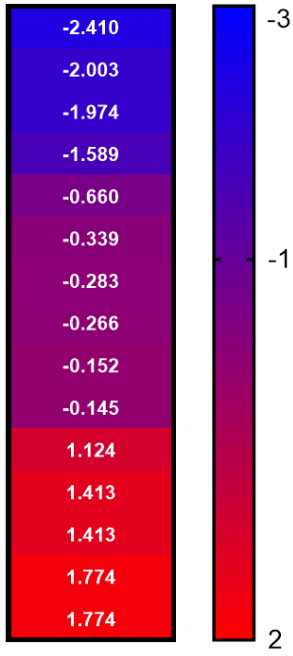

	p-value	Activation Score
Proliferation of neuroglia	0.00193	-0.314
Formation of dendritic spines	0.0147	0.577
Formation of dendrites	0.0284	0.577
Growth of dendrites	0.00487	1.082
Dendritic growth/branching	0.000413	1.090
Density of dendritic spines	0.02	1.165
Axonogenesis	0.0156	1.412
Branching of neurons	5.32E-05	1.587
Proliferation of neural cells	0.00537	1.627
Neuritogenesis	5.03E-06	1.913
Branching of axons	0.00933	1.922
Branching of neurites	0.000164	1.924
Outgrowth of neurites	0.0169	1.988
Growth of neurites	0.0122	2.238
Development of neurons	1.27E-06	2.286

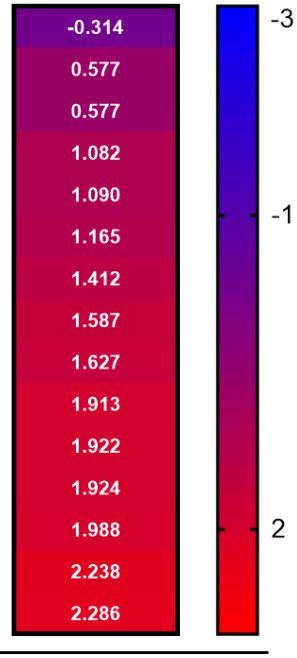

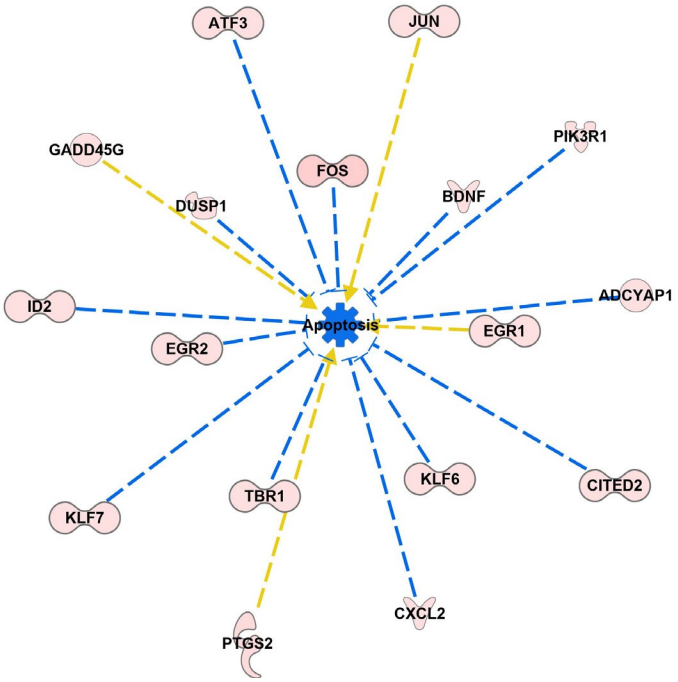

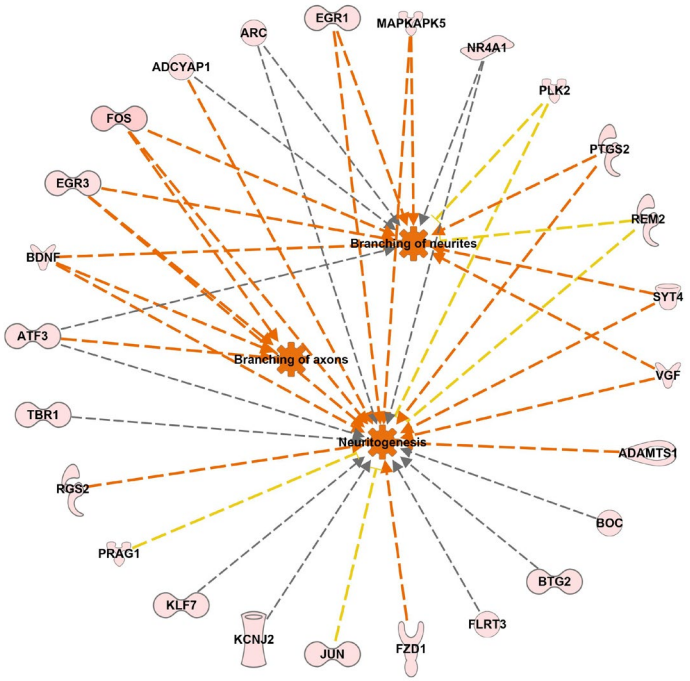

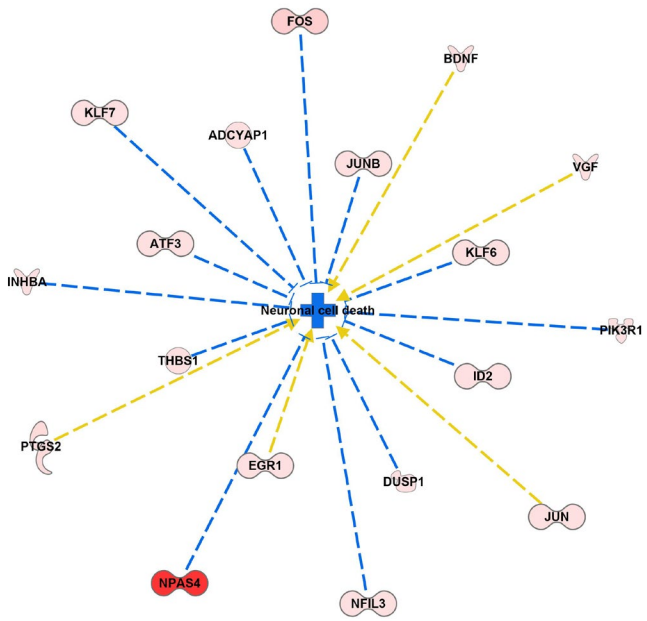

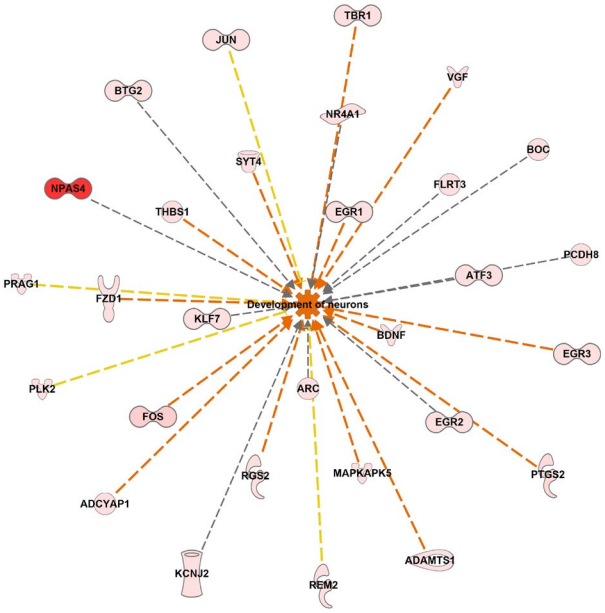

4A.

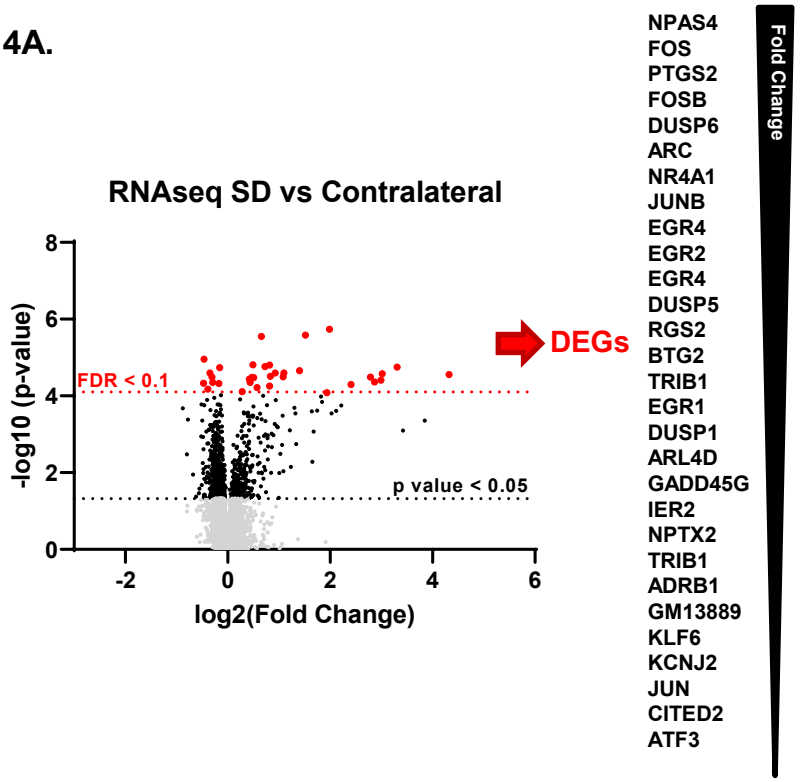

4B.

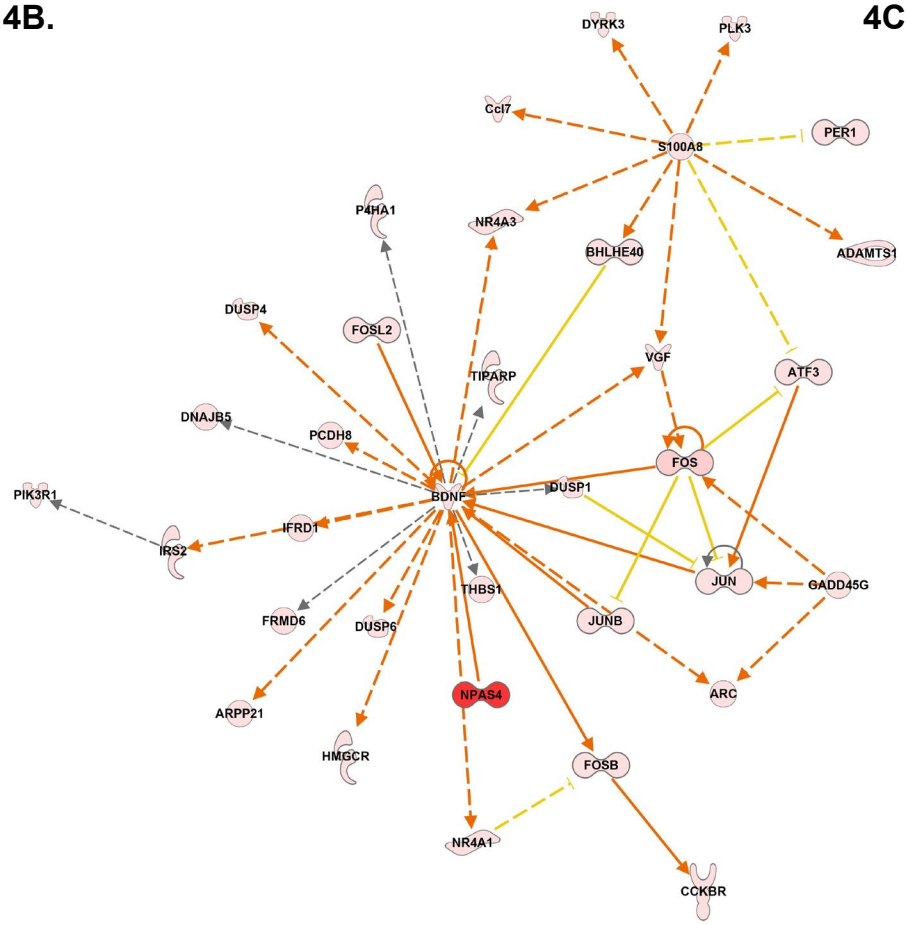

4C.

Disease and Disorders	p-value range	# Molecules
Neurological Diseases	4.56E-02 - 2.49E-08	73
Organismal Injury and Abnormalities	4.56E-02 - 1.91E-08	73
Psychological Disorders	2.85E-02 - 1.91E-08	35
Hereditary Disorders	1.54E-02 - 1.91E-08	21
Skeletal and Muscular Disorders	7.75E-03 - 6.30E-08	20

Physiological System Development and Functions	p-value range	# Molecules
Nervous System Development and Function	4.56E-02 - 7.04E-07	61
Tissue Morphology	4.56E-02 - 1.07E-09	39
Tissue Development	4.56E-02 - 1.03E-06	49
Organismal Development	4.56E-02 - 5.03E-06	44
Organ Morphology	4.56E-02 - 5.96E-05	16

	p-value	Activation Score
Cell death of hippocampal neurons	0.0015	-1.958
Apoptosis	9.12E-08	-1.197
Neuronal cell death	8.64E-06	-0.903
Cell death of cerebral cortex cells	0.00133	-0.838
Apoptosis of neuroglia	0.00107	-0.152
Apoptosis of sympathetic neuron	6.08E-05	-0.145
Apoptosis of granule cells	0.000199	0.063
Cell death of cortical neurons	0.0346	0.173
Cell viability of cerebral cortex cells	0.00112	1.126
Survival of cephalic neurons	0.00112	1.126
Survival of neural cells	0.0188	1.475
Cell viability	0.0203	1.475

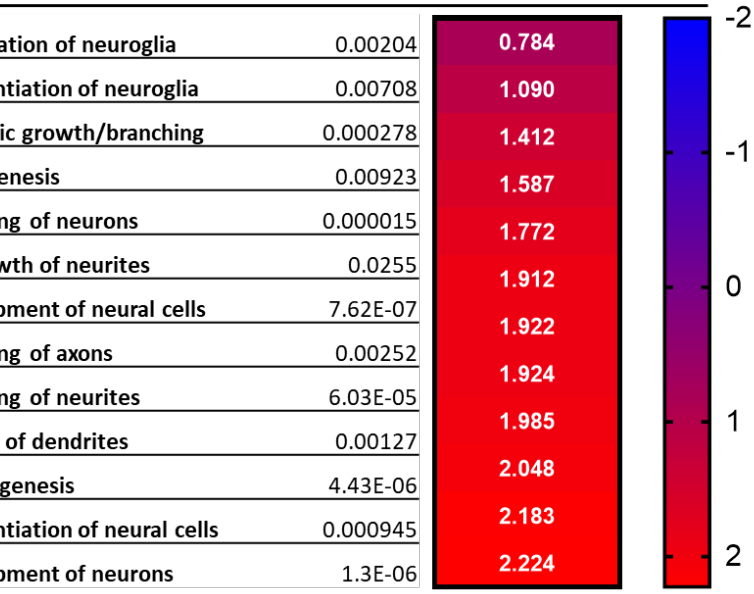

	p-value	Activation Score
Proliferation of neuroglia	0.00204	0.784
Differentiation of neuroglia	0.00708	1.090
Dendritic growth/branching	0.000278	1.412
Axonogenesis	0.00923	1.587
Branching of neurons	0.000015	1.772
Outgrowth of neurites	0.0255	1.912
Development of neural cells	7.62E-07	1.922
Branching of axons	0.00252	1.924
Branching of neurites	6.03E-05	1.985
Growth of dendrites	0.00127	2.048
Neuritogenesis	4.43E-06	2.183
Differentiation of neural cells	0.000945	2.224
Development of neurons	1.3E-06	

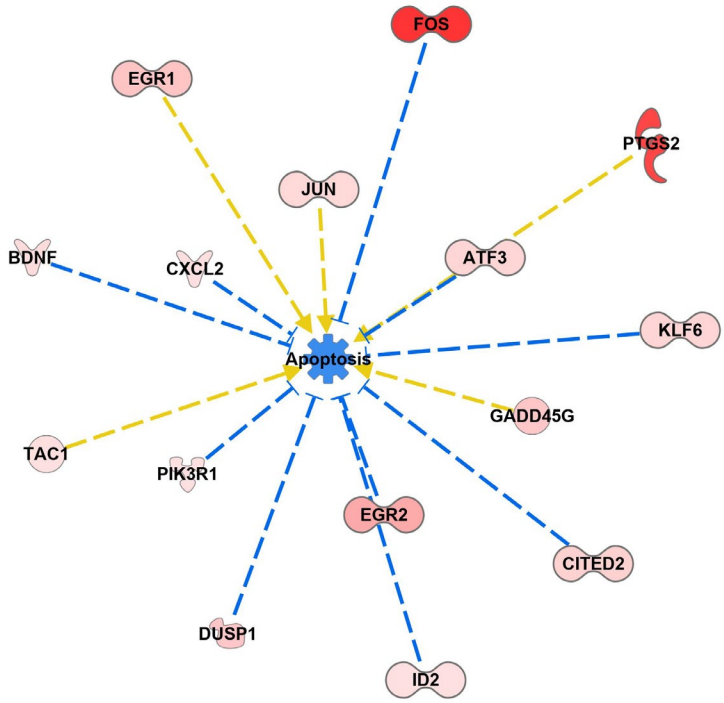

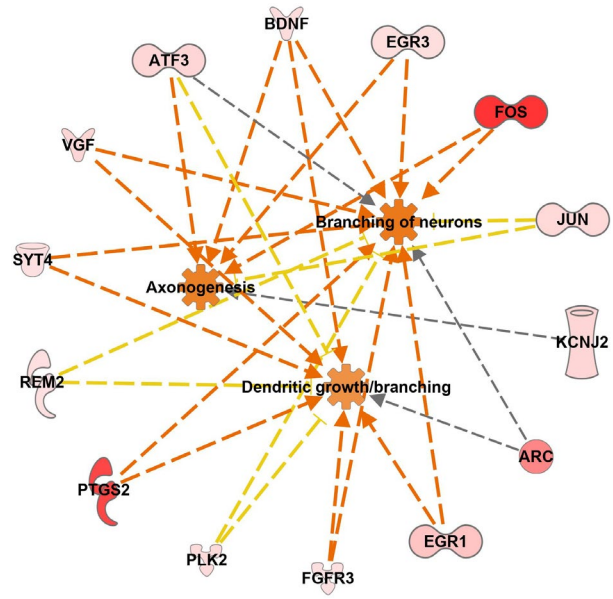

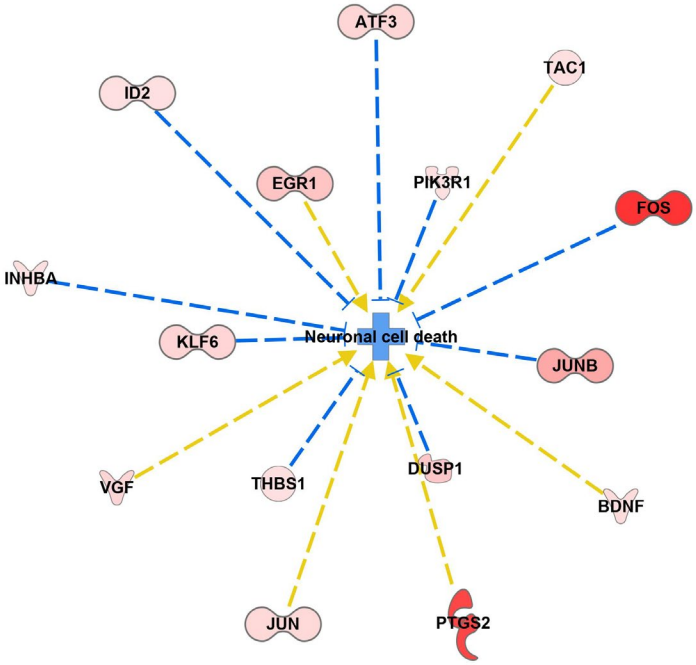

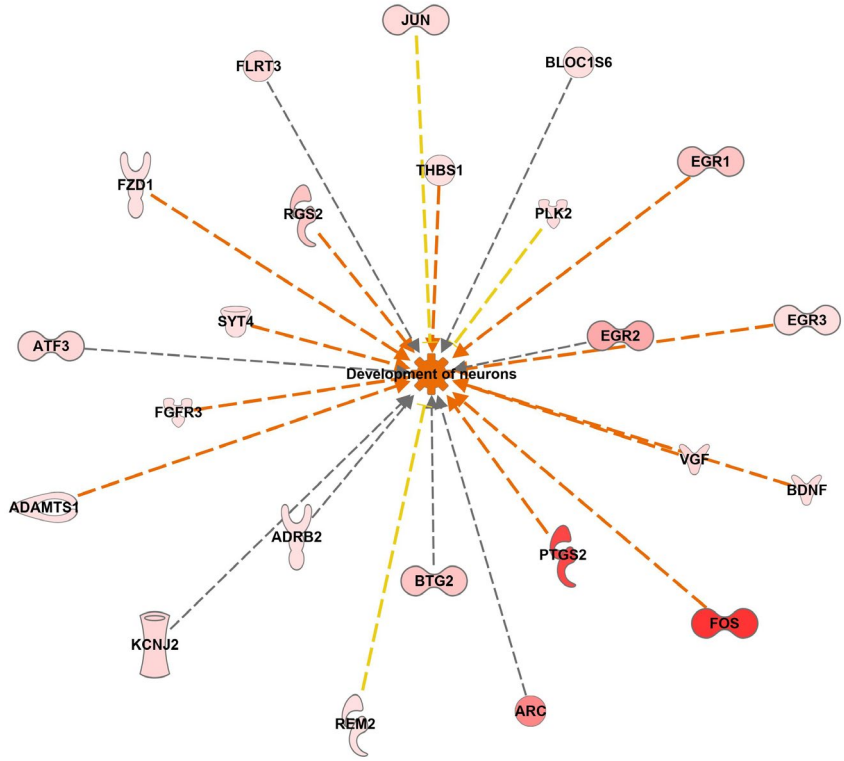

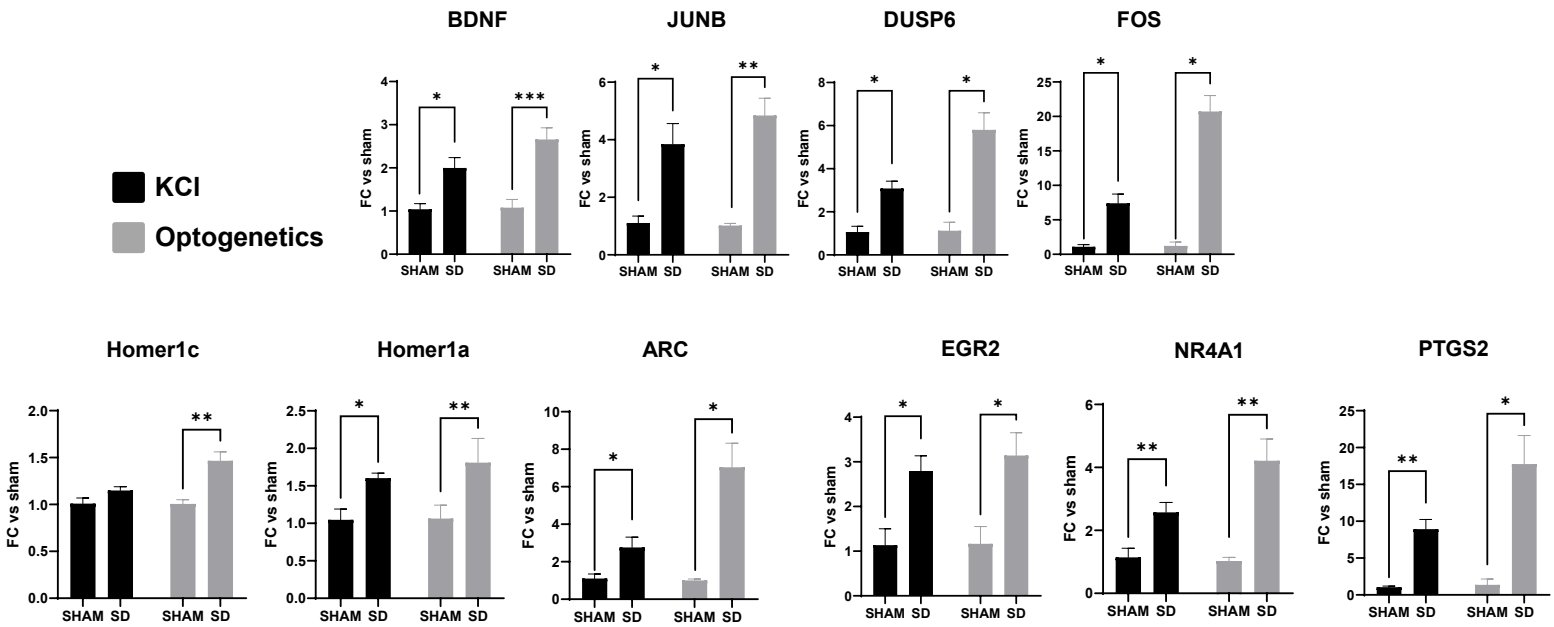
KCl
Optogenetics
BDNF
JUNB
DUSP6
FOS
Homer1c
Homer1a
ARC
EGR2
NR4A1
PTGS2
FC vs sham
SHAM SD
SHAM SD

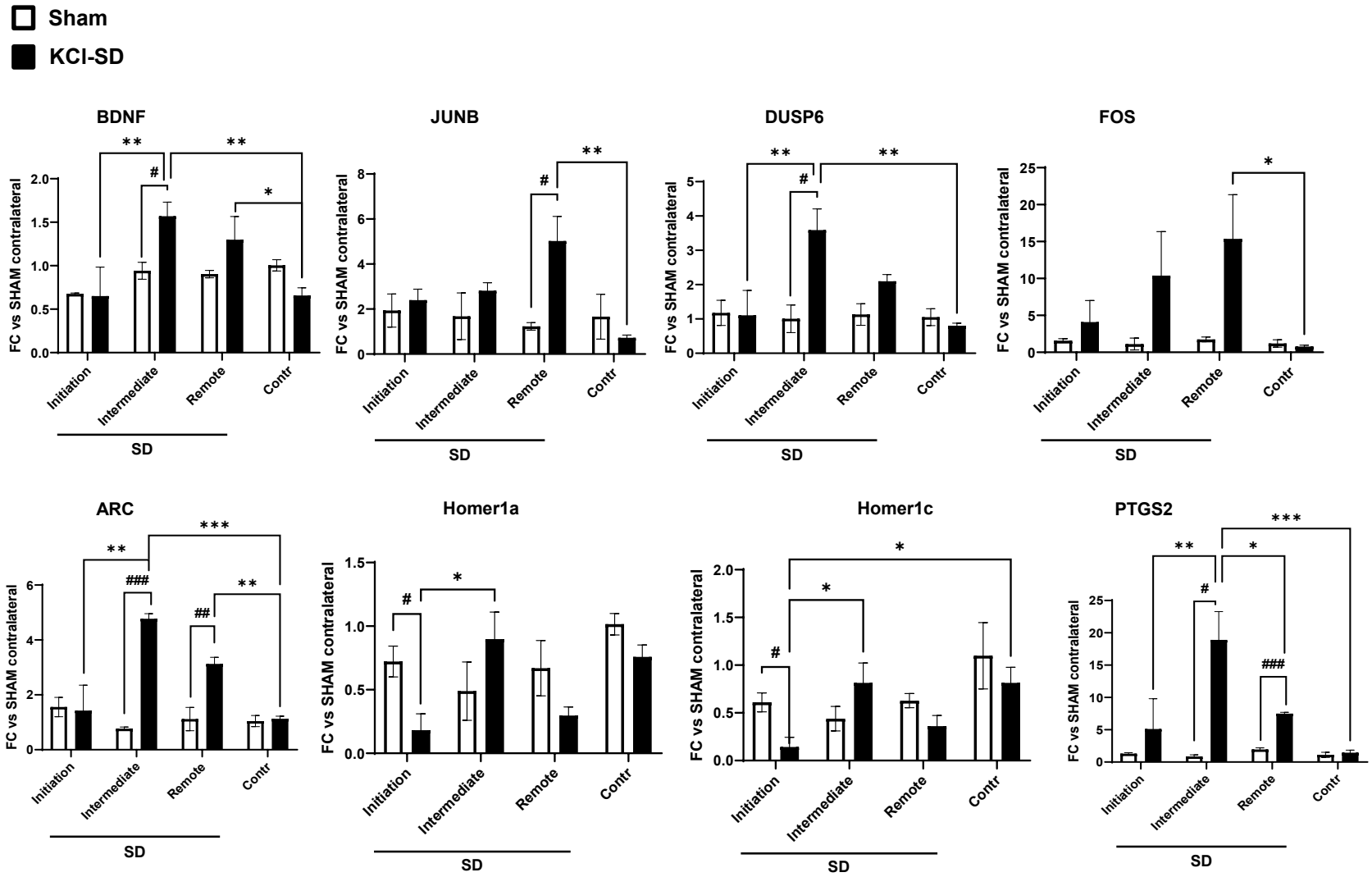
Sham
KCI-SD
BDNF
JUNB
DUSP6
FOS
ARC
Homer1a
Homer1c
PTGS2
FC vs SHAM contralateral
Initiation
Intermediate
Remote
Contr
SD

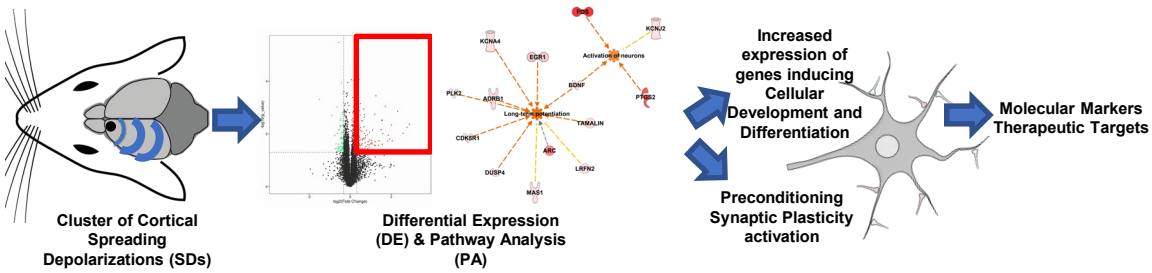
Cluster of Cortical Spreading Depolarizations (SDs)
Differential Expression (DE) & Pathway Analysis (PA)
KCNA4
EGR1
KCNJ2
Activation of neurons
PLK2
ADRB1
BDNF
PTGS2
Long-term potentiation
TAMALIN
CDKSR1
ARC
DUSP4
LRFN2
MAS1
Increased expression of genes inducing Cellular Development and Differentiation
Preconditioning Synaptic Plasticity activation
Molecular Markers Therapeutic Targets

1A.

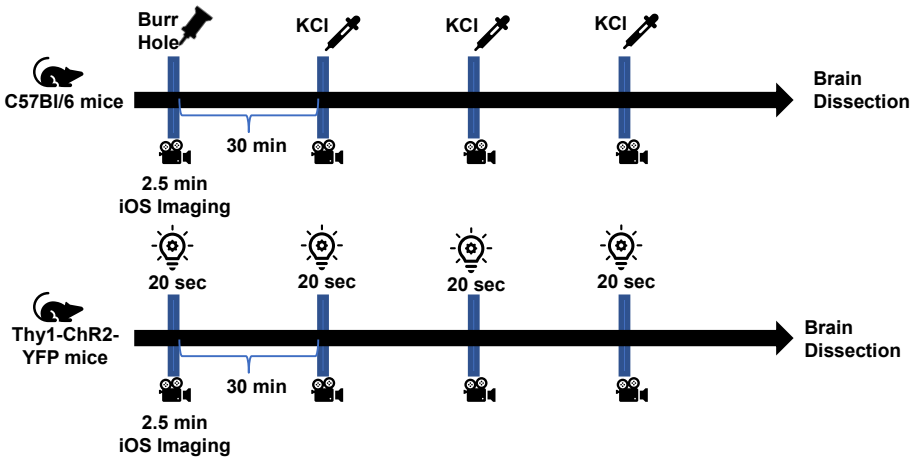
Burr Hole
KCl
KCl
KCl
C57Bl/6 mice
Brain Dissection
30 min
2.5 min iOS Imaging
20 sec
20 sec
20 sec
20 sec
Thy1-ChR2-YFP mice
Brain Dissection
30 min
2.5 min iOS Imaging

1B.

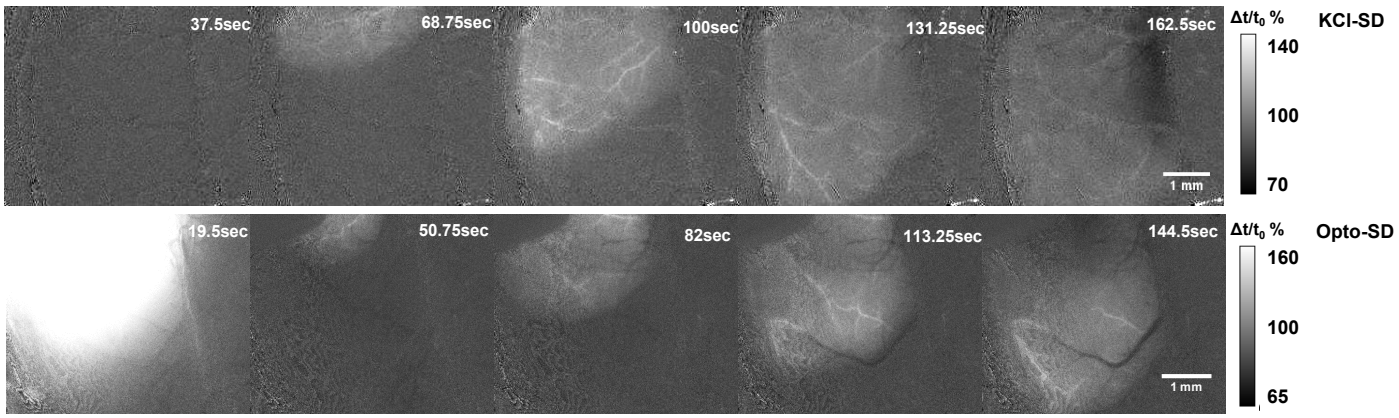
37.5sec
68.75sec
100sec
131.25sec
162.5sec
Δt/t0 %
KCl-SD
140
100
70
1 mm
19.5sec
50.75sec
82sec
113.25sec
144.5sec
Δt/t0 %
Opto-SD
160
100
65
1 mm

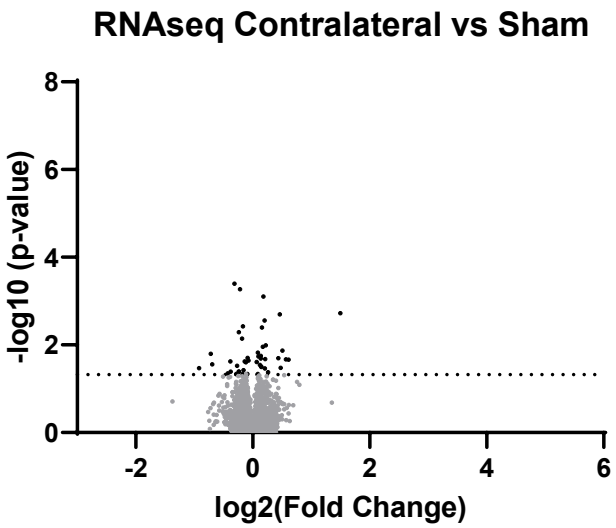
RNAseq Contralateral vs Sham
-log10 (p-value)
8
6
4
2
0
-2
0
2
4
6
log2(Fold Change)

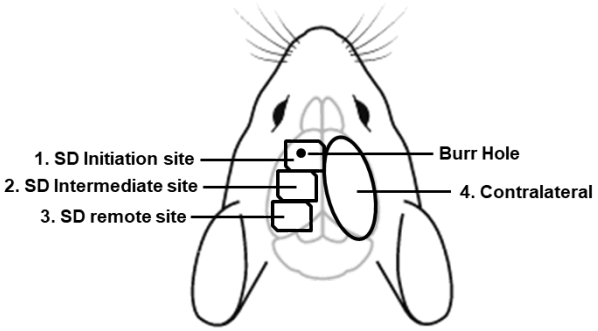
1. SD Initiation site
2. SD Intermediate site
3. SD remote site
Burr Hole
4. Contralateral

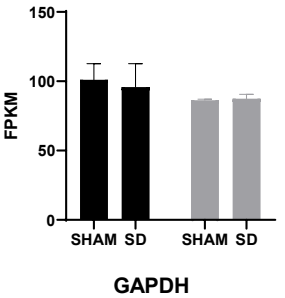
FPKM
150
100
50
0
SHAM SD
SHAM SD
GAPDH

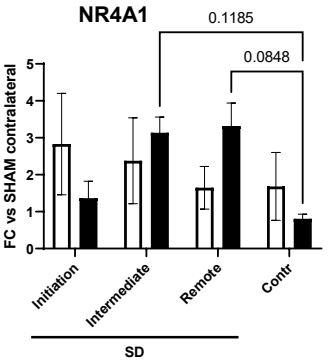
NR4A1
0.1185
0.0848
FC vs SHAM contralateral
5
4
3
2
1
0
Initiation
Intermediate
Remote
Contr
SD

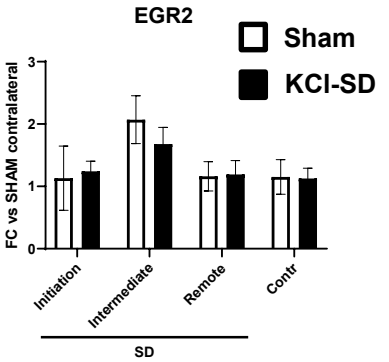
EGR2
Sham
KCl-SD
FC vs SHAM contralateral
3
2
1
0
Initiation
Intermediate
Remote
Contr
SD